第2部　歯槽骨再生方法の開発：OstemiR（オステミア）の同定

A. 研究目的

ゲノムからの転写産物の多くは，複数のステム，ループ，バルジ構造をとるが，それらのうちいくつかがmicroRNA前駆体(primary miRNA, pri-miRNA)をなす．哺乳類では，RNaseIII であるDrosha タンパク質による切断によって，pri-miRNA からより単純なステム・バルジ・ループ構造をもつ pre-miRNA が発生する．その後Exportin-5 によって細胞質へと輸送される(Grimm and Streetz, 2006; Diederichs and Jung, 2008). さらに pre-miRNA は，やはりRNaseIII であるDicer 複合体によってループ部分が切断除去されることで二本鎖 RNA 構造が生成される．二本鎖 miRNA の各鎖すなわち一本鎖 mature miRNA あるいは siRNA は，およそ 20-30 ヌクレオチドの一本鎖 RNA であり，Argonaute タンパク質とRNA-induced silencing complex (RISC)を形成し (Siomi H and Siomi MC, 2009)，特定のmRNA との部分的なハイブリダイゼーションにより，特定の mRNA からタンパク質への翻訳の抑制(Olsen and Ambros, 1999)，mRNA の分解誘導(Hatvagner and Zamore, 2002; Llave and Xie, 2002) を行う．加えて，エクソソームの中にもmiRNA が存在することが知られてきた(Hu and Drescher, 2012)．

発生過程における骨形成および成体における骨代謝にとって，骨芽細胞および骨細胞は主要な役割を担う細胞である．骨芽細胞は，多能性をもつ未分化間葉系幹細胞に由来する(Harada and Rodan, 2003)．骨芽細胞は，さらに最終分化段階である骨細胞へと成熟し，骨マトリックスの中で個々の骨細胞はラクナと呼ばれる穴に存在する(Aarden and Burger, 1994)．この分化と成熟は，骨芽細胞分化のマスター転写因子としてこれまでに Runx2/Cbfa1, Sp7/Osterix, beta-catenin が知られてきた(Karsenty and Kronenberg, 2009; Komori T, 2006). また骨芽細胞分化を促進する成長因子として BMP ファミリーや CCN ファミリーが知られている (Perbal and Takigawa, 2005; Kubota and Takigawa, 2011). これまでに，Runx2(Zhang and Xie, 2011), FAK (Eskildsen and Taipaleenmaki, 2011), Connexin43 (Inose and Ochi, 2009)のそれぞれの mRNA を直接認識することによって骨芽細胞分化を制御するmiRNA が示されてきた．

骨芽細胞分化の研究には，MC3T3-E1 (MC3T3), C3H10T1/2, ST2, C2C12, KUSA-A1 (KUSA) および実験動物およびヒトからのプライマリー細胞が用いられてきた．これらのうちKUSA 細胞は培養皿中で旺盛に増殖し，豊富なALP 活性，骨グラタンパク質(bglap/osteocalcin)の産生，石灰化を示し，Sca-1, CD44, Ly-6C, CD140 といった細胞表面マーカーを発現する(Ochi and Chen, 2002; Kawashima and Shindo, 2005)．さらに，KUSA 細胞をマウス皮下に注射すると異所性骨化を誘発した．また，骨細胞の単離と培養が困難であることから有用な骨細胞株は少なく，プライマリー細胞が利用されてきた(Kato and Windle, 1997; Kamioka and Honjo, 2001)．既知の骨細胞マーカーとしては，DMP1, FGF-23, Sclerositin が知られている(Franz-Odendaal and Hall, 2006; Ikeda, 2008). 分泌タンパク質であるDMP1 が最初に発表された骨細胞マーカーである(Toyosawa and Shintani, 2001). FGF-23 は，腎臓におけるリンの排泄とビタミンDの活性化を調節することで生体のミネラルの恒常性を維持するという重要な生理的機能をもつ(Lorenz-Depiereux and Bastephe, 2006; Feng and Ward, 2006;)．硬結性硬化症(Sclerosteosis)の原因遺伝子である sost にコードされるSclerostin もまた骨細胞マーカーである(Bezooijen and Roelen, 2004; Winkler and Sutherland, 2003).

本研究では，半網羅的な miRNA Array 解析を援用することによって，KUSA 細胞の骨細胞分化過程における miRNA 発現変動パターンを明らかする．それらの miRNA のうち特徴的な発現変動を示す miRNA を抽出し，骨細胞分化関連因子との関わりを探った．

B. 研究方法

細胞培養と分化誘導

マウス骨髄間質由来 KUSA-A1(KUSA)細胞とマウス頭蓋冠由来MC3T3-E1 (MC3T3)細胞は，理研細胞バンクより供与を受けた(Ochi and Chen, 2002)．これらの細胞株は10%血清を含むDMEM 中で，5%二酸化炭素濃度で培養された．細胞はコンフルエントまで培養され，L アスコルビン酸，デキサメタゾン，ベータグリセロフォスフェートが2日おきに添加された．

カルシウム沈着の染色

アリザリンレッド染色は，通法に従い実施された(Kawata and Eguchi, 2006)．

RNA の調製

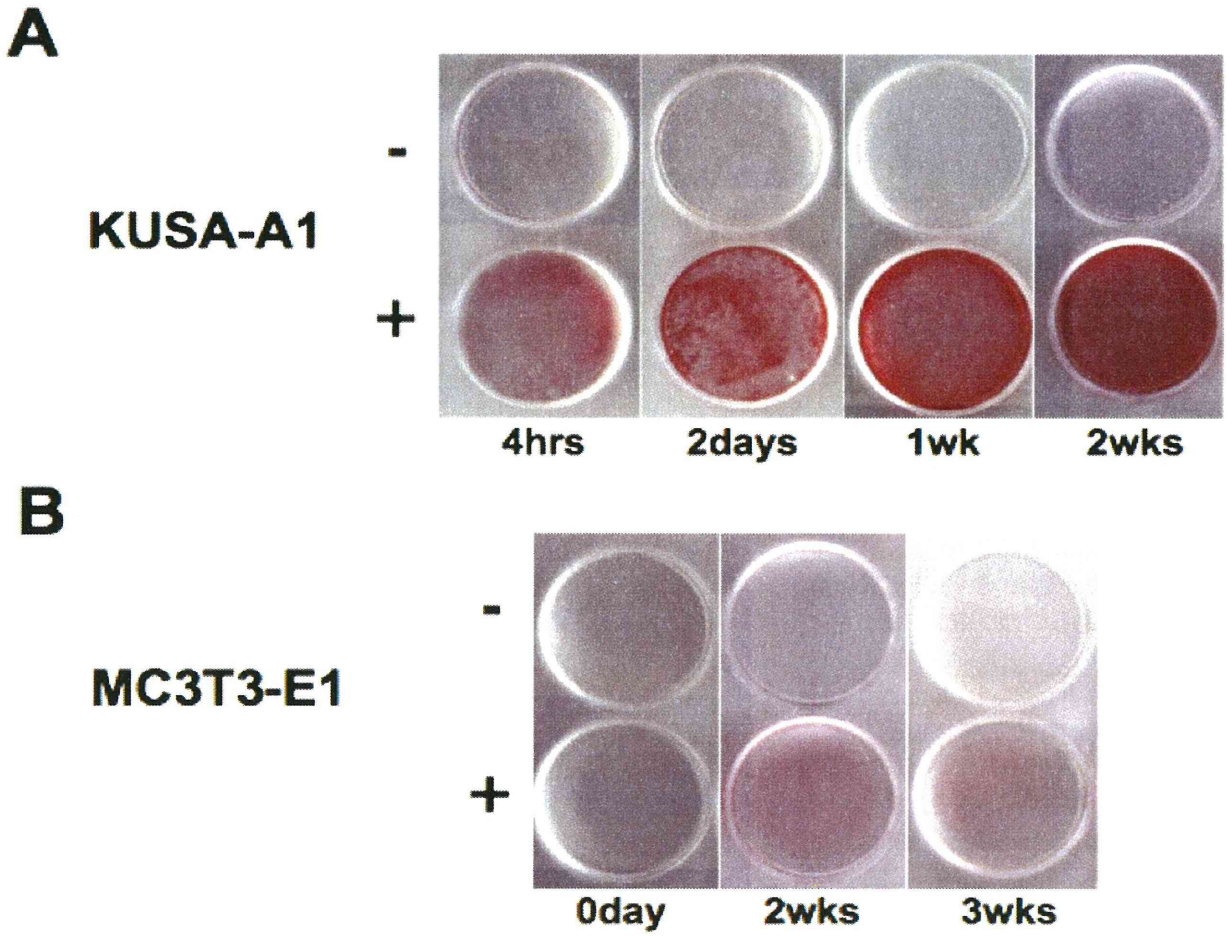

図1. KUSA-A1 (A)および MC3T3 (B)の骨芽細胞分化過程におけるアリザリンレッド染色.

低分子 RNA を含むトータル RNA の調製は, miRNeasy mini kit(キアゲン)を用い, DNase 処理とともに行った.

miRNA qPCR アレイ

アダプターを援用した cDNA 合成は RT2 first strand kit (SABiosciences) を用いて行った. miRNA qPCR アレイは, miFinder miRNA PCR array を用いて行った. miScript array data analysis (SABioscience) を用いて, ヒートマップ解析(2 サンプル比較)、クラスタグラム解析(多数サンプル比較)、スキャッタープロット解析(2 サンプル比較)を行った。

プライマーのデザインと qRT-PCR

cDNA は上記方法あるいは All-in-One miRNA qRT-PCR kit (Gene Copoeia)を用いて合成した. 各 mature miRNA に特異的なプライマーは, miRBase における一次及び二次構造に基づいて設計した(Griffiths-Jones and Saini, 2008).

miRNA を定量するための qPCR は, SYBR Premix Ex Taq (TaKaRa)を用いて行った. qRT-PCR による mRNA の定量は通法に従い行った (Eguchi and Kubota, 2008).

miRNA のターゲット予測

TargetScan を援用した(Lewis and Burge, 2005).

統計

細胞は, デュプリケートあるいはトリプリケートで培養され実験に用いられた. リアルタイム PCR はトリプリケートで行われ, 平均値が算出され用いられた. 標準偏差は, 独立した培養皿のデータをもとに算出された.

(倫理面の配慮)

当該研究課題では、ヒトならびにヒト組織由来試料ならびに実験動物を使用していない。

C．研究結果

KUSA 細胞の骨細胞分化

骨細胞分化のモデルとして，KUSA 細胞とMC3T3 細胞の有用性を検討した(図1)．分化誘導サプリメントを添加することによって，KUSA 細胞では添加の4時間後から2週間後にかけて段階的なカルシウムの蓄積を認め，石灰化が立証された(図1A)．このカルシウムの蓄積は KUSA 細胞においては2週間後に顕著であったが，MC3T3 細胞では大変緩やかであった(図1B)．

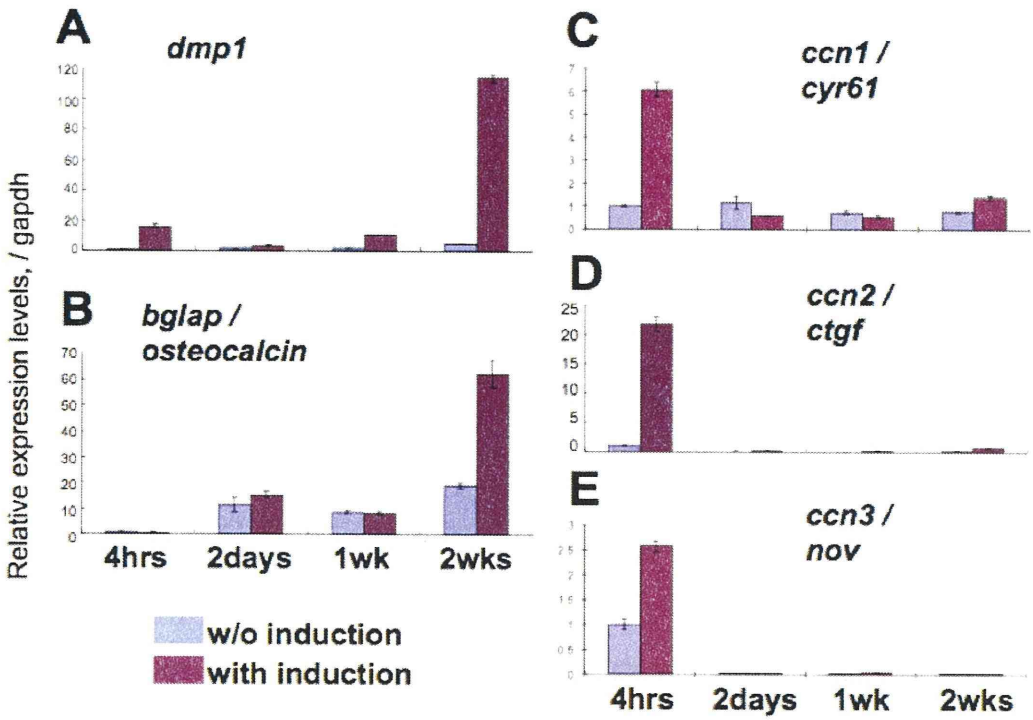

図2. KUSA-A1 細胞の分化過程における遺伝子発現変化．Dmp1 (A) 及び bglap/osteocalcin (B) の mRNA は骨細胞マーカーとして定量された．Cyr61/ccn1 (C)，ctgf/ccn2 (D) 及び nov/ccn3 (E) の mRNAs は，骨芽細胞と軟骨細胞のマーカーとして定量された．

細胞の分化段階についての確証を得るために，分化マーカーの定量を行った．骨細胞マーカーである Dmp1 は，KUSA 細胞の段階的な石灰化の間に，顕著に誘導された(図2A)．もう一つの骨細胞マーカーである Bglap/オステオカルシンは，分化誘導開始の2週間後に誘導が確認された(図2B)．加えて，CTGF，Cyr61，Nov といった CCN ファミリーのメンバーが最初の分化刺激によって誘導された(図2C，D，E)．これらの結果から，KUSA 細胞が骨細胞分化研究のモデルとして有用であることが再確認された．

miRNA アレイの概要

骨細胞分化と細胞の幹性(stemness)を制御する新規の miRNA の探索のために，qRT-PCR を基本とした miRNA アレイを使用した．概要として，骨細胞分化誘導2週間での miRNA 発現レベルは，他の実験条件(誘導前および対象実験)と比較して全体的に低かった(図3A)．別の表現を使うと，ほとんどの miRNA は，KUSA 細胞の未成熟な段階と比べて成熟した骨細胞の段階において低く発現していた(データ略)．骨誘導の2週間後に発現低下した miRNA には let-7a ファミリーおよび miR-30 ファミリー (miR-30a/d/e) が含まれていた(データ略)．

次に定量した全 miRNA をクラスタグラムによって解析した(図3B)．クラスタグラムの結果に基づき，miRNA を8種類に分類した(データ略)．最も主要な miRNA 群は，骨誘導なしの2週間培養によって発現が上昇した miRNA 群であった．

オステミアについてより理解するために，2つの実験群間における miRNA の発現レベルを比較したヒートマップを作成した．miR-30d の発現レベルは，4h-の条件と比較した場合，4h+，2w-，2w+のいずれの条件においても高かった(図4A-C)．骨誘導のための一度の刺激によっ

て，miR-30d だけでなく miR-155 も誘導された（図4A）．miR-16 の発現レベルは，同様の単刺激によって減少した（図4A）．骨誘導の反復刺激によって，miR-30d と miR-30c が誘導され，miR-503，miR-322，miR-125-3p の発現レベルは最も抑制された（図4B）．miR-30d と miR-150 は，他の miRNA と同様に2週間の長期培養によっても発現誘導された（図4C）．miR-503 および miR-744 は長期培養によって減少した．

miRNA 発現の標準化された定量

KUSA の骨細胞分化における miRNA 定量のための内部標準を決定するために，Snord85，Snord66，Rnu6，miRTC，PPC の発現パターンを miRNA アレイの結果から抽出した（図5A）．それらのうち Snord66 と PPC の発現パターンは各実験条件間において最も安定しており，Rnu6 と Snord85 の発現パターンは安定していなかった．従って，Snord66 と PPC をその後の KUSA 骨細

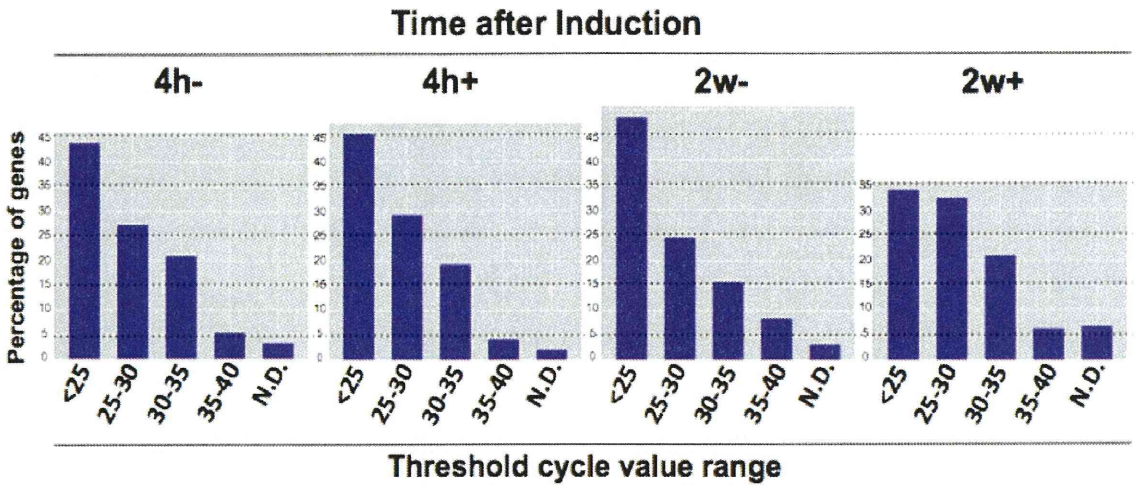

図3．各実験条件間での miRNA 発現傾向の相違．

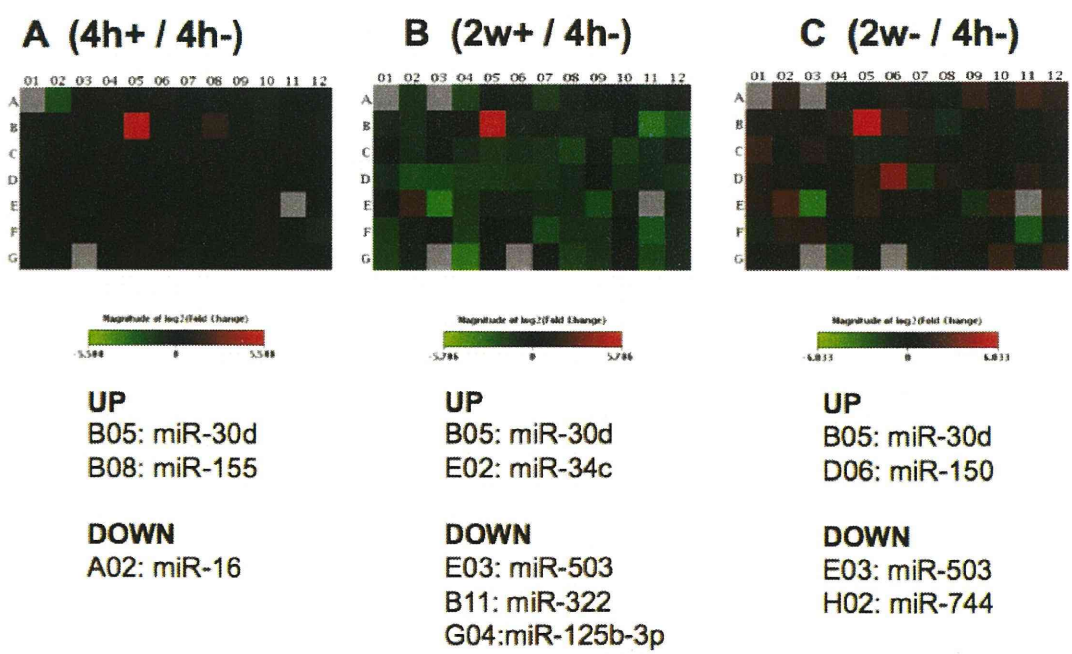

図4．miRNA アレイ及びヒートマップ解析．発現上昇は赤，発現低下は緑で示した．骨誘導の4時間後（4h+，A），2週間の骨誘導（2w+），2週間の長期培養（2w-）の各 miRNA 発現量は，無刺激の miRNA 発現量（4h-）と相対比較された．

胞分化実験における miRNA 定量の内部標準として適用した.

次に, miRNA アレイの結果の信憑性について確認するために, 各 miRNA に対する特異的プライマーを設計し, それらを用いて qRT-PCR を行った. miR-21 および miR-155 の発現は, qRT-PCR によっても miRNA アレイによっても最初の刺激によって上昇したものの, 最終分化段階においては抑制された. miR-322 についても同様の方法で検討し, qRT-PCR および miRNA アレイの両方において, 骨誘導の2週間後の時点で発現の低下を示した(データ略). miR-16 が骨細胞ステージにおいて抑制されるとの結果は, qRT-PCR によっても miRNA アレイによっても確認された(データ略). miRNA アレイの結果, miR-30d は単刺激, 複数回刺激, 長期培養のいずれでも誘導されるとの結果を得たものの, qRT-PCR の結果では単刺激のみによって誘導されるとの結果を得た(データ略).

オステミア(ostemiR)のターゲットおよび機能の予測

骨細胞分化の過程で顕著に発現変動した miRNA の機能とターゲットについて, 予測及び推察を行った(表2). これらのオステミアは, 骨形成あるいは細胞の幹性に関わる遺伝子をターゲットとすると予測された. エピジェネティクス関連遺伝子もまたオステミアのターゲットであると予測された. 骨細胞分化の間に上昇した一群の miRNA, すなわち miR-30d, miR-155, miR-21, miR-16 を含む miRNA 群は, 骨形成マーカーであると同時に, 骨芽細胞の幹性の維持を抑制する可能性がある. miR-34c と miR-16 はいずれも骨細胞ステージである 2w+で上昇したため, 骨細胞マーカーであると同時に, 骨芽細胞維持遺伝子を抑制する可能性がある.

骨制御因子をターゲットとする miRNA の予測

骨制御因子をターゲットとする miRNA の予測によって, 脊椎動物間で保存された, 哺乳類のみで保存された, あるいは種間であまり保存されていない miRNA 認識部位が各 3'非翻訳領域上に予測された. 以下では脊椎動物間で保存された, あるいは哺乳類で保存された miRNA にのみについて論ずる. 骨細胞マーカーである Dmp1 の 3'非翻訳領域を認識する miRNA として, let-7/miR-98 が予測された(データ略). let-7 ファミリーの全メンバーは, 骨細胞分化の過程で発現抑制されたことから, let-7 ファミリーの低下は dmp1 遺伝子の発現抑制を解除することが示唆された. さらに, 骨形成因子である ctgf/ccn2 の 3'非翻訳領域を認識すると予測された miRNA の中でも, miR-18ab と miR-19 は骨細胞分化の過程で上昇するオステミアでもあった.

骨芽細胞最終分化と転写因子群

骨芽細胞分化において Runx2 や Osterix が必須の役割を担っていることはすでに明らかになっているが, 後期の分化(骨細胞への最終分化)については未知である。そこで、MC3T3 の長期培養において発現誘導される転写因子の検索を行った。骨細胞分化のマーカー

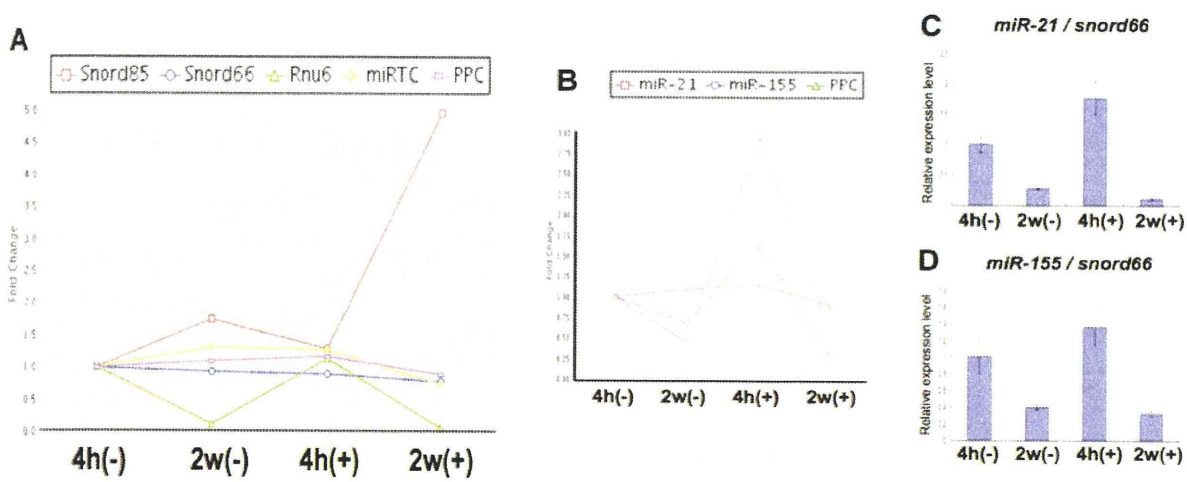

図5. 骨細胞分化過程における miRNA の発現定量. (A) miRNA 発現定量のための内部標準の検討 . (B) miRNA アレイによる miR-21 及び miR-155 の発現変動. (C, D) リアルタイム PCR による miR-21 及び miR-155 の発現変動. 内部標準として Snord66 を用いた.

として、sost, phex, mepe の遺伝子発現を指標にして、MC3T3 細胞を 7 週間分化培養し，これらの遺伝子群発現を確認した。この過程で、dlx3, mef2c, tcf7 といった転写因子群の発現亢進が顕著であることを見いだした。そこで、これらの転写因子群の強制発現ならびにノックダウンによる機能亢進と機能減少による骨芽細胞最終分化のプロファイリングを行ったところ、Dlx3 強制発現系で骨細胞分化が亢進し、また、Mef2c と Tcf7 の強制発現では部分的に分化が亢進した。一方，Dlx3, Mef2c, Tcf7 のいずれのノックダウンでも骨芽細胞最終分化は抑制された。骨芽細胞分化での必須な役割について既知である Runx2, Osterix の強制発現発現では、Runx2 は骨芽細胞後期分化において抑制、Osterix は亢進した。これらのノックダウンは両者とも骨芽細胞の分化形態が低下し、それに伴い後期分化も低下した。

D. 考察

本研究では，まず KUSA 細胞を活用して，骨芽細胞が骨細胞に成熟する実験系を確立した．Osteocytogenesis における miRNA の半網羅的な発現解析によって，Osteocytogenesis に伴い特徴的に発現変動する一群の miRNA が明らかとなりそれらを OstemiR と命名した．その一部を，個別の定量 PCR で解析し，miRNA PCR Array と個別の PCR との間で類似した結果を得た．OstemiR のターゲット予測の結果，骨形成に必須の転写因子である Runx2 やパターン形成に必須の成長因子 Wnt family などが予想された．またエピジェネティクスに関わる遺伝子も OstemiR のターゲットとして予想された．骨形成に関わる dmp1, ctgf, runx2 および osterix の 3' 非翻訳領域探索の結果，miRNA Array で抽出した OstemiR が dmp1, ctgf, runx2 および osterix を標的とすることが予測された．

骨細胞分化研究における KUSA 細胞の有用性

骨芽細胞分化モデルとして KUSA 細胞および MC3T3 細胞を検討した（図1）．その結果，KUSA 細胞では顕著かつ段階的な石灰化および dmp1 と bglap/ocn の発現上昇を認めた．また分化誘導初期に CTGF/CCN2, Cyr61/CCN1, Nov/CCN3 といった CCN 遺伝子ファミリーの顕著な発現上昇を認めた．これに対し，MC3T3 では僅かな石灰化しか認めなかった．このように骨髄間質細胞である KUSA 細胞が，今回用いたサプリメントによって綺麗に骨細胞まで分化誘導したのに対し，頭蓋骨由来である MC3T3 は今回の分化誘導とマッチしなかったと考えられた．これらの結果から，KUSA 骨細胞分化系は，骨研究のために有用であることが分かった．

miRNA Array および定量 PCR によるオステミアの抽出

次に，miRNA Array によって半網羅的解析を行った結果，まず骨細胞分化ステージである 2w+では，他の実験条件と比較してほとんどの miRNA の発現が低下し，それらには Let-7 family および miR-30a/d/e が含まれていた（図3，表1）．従って，miRNA の総量が骨細胞では低下すると考えられる．このことは，第一に，多くの遺伝子の翻訳抑制の解除が起こることを意味す

miRNA	Results in arrays	Results in qRT-PCR (M)	Possible actions	Possible target signals	TargetScan, bone- and stem-related	TargetScan, epigenetic and others
miR-30d	Low in 4h-	High in 2h+	Repressing stemness or osteoblast factors	Wnt, FGF, BMP/ TGFb, Runx2, Osx	RUNX2, SOX9, LRP6, SMAD2, SMAD1, NOTCH1, NOV TET1,TET3,	ITGA4, MLL, SNAI1, JMJD1A, ITGB3, SIRT1, HDAC5, ITGA5, NCOA1, HOXB8,IGF, FOXO3, SENP5, MBD6, IGF2R, IGF1R, KLF9, KLF11, ZEB2, BDNF, HSPA5,
miR-155	High in 4h+, Low in 4h-	Similar	Repressing stemness or osteoblast factor	Wnt, FGF, BMP/ TGFb, Runx2, Osx	LRP1B, TCF4, SP1, SMAD2,GDF6, FGF7, FOS, SMAD1, SP3, TGFBR2, ACVR2B,	JHDM1D, TP53INP1, JARID1B, SIRT1, SMARCAD1, KLF3, DNAJB1, Claudin-1,
miR-21	High in 4h+, Low in 4h-	Similar	Repressing stemness or osteoblast factor	Wnt, FGF, BMP/ TGFb, Runx2, Osx	BMPR2, ACVR1C, SKI, LIFR, TGFBI, SOX5, FGF1, SMAD7, LRP6, KLF5, SOX2, TGFBR2, MSX1, TET1,	RECK, ITGB8, KLF3, JHDM1D, TIMP3, KLF12,
miR-34c	High in 2w+, low in 4h-		Repressing stemness or osteoblast factor	Wnt, FGF, BMP/ TGFb, Runx2, Osx	MYCN, FGF23, NOTCH1/2, ACVR2B, SMAD4, FOSB	HSPA1B, CTNND2, BCL2, JHDM1D, ITGB8, ITGA10, TGIF2, PDGFRA,
miR-16*	High in 4h-, Low in 4h+/2w+	Low in 2w+	Repressing stemness or osteoblast factors	Wnt, FGF, BMP/ TGFb, Runx2, Osx, CCN	INSR, ACVR2B, SMURF1, FGF7 ,LRP2/6, FGFR1, SMAD7, WNT3A, NOTCH2, SMAD5, SMAD3, IHH, WNT4, TGFBR3, LRP1B, TCF3, SMURF2, BMPR1A, IGF2R, WNT7A, BMP8A, WISP1, SOX5, WNT5B, ACVR2A	MYB, GFAP, SIRT4, MYBL1, VEGFA, RECK, BDNF, HSPG2, SUMO3, ITGA10,LITAF, FOXO1,CREBZF, CTNNBIP1, FOSL1, TET3, IGF1R, IGF1, GHR, RICTOR, CLDN2, DNAJB4, PTH,
miR-322/424*	High in 4h-, Low in 2w+	High in 4h+, Low in 2w+				
miR-503	High in 4h-, Low in 2w+/-		Repressing stemness or osteoblast factors	BMP/TGFb, Runx2, Osx, CCN	SMURF1, FGF7, INSR, ACVR2B, BMPR1A, SMAD7, SMURF2, WNT3A, WNT4, SOX5, IHH	RECK, JARID2, VEGFA, MYBL1, FOSL1, HSPG2, IGF1, IGF1R,
miR-541						
miR-744	High in 2w+/-, Low in 4h-		Repressing stemness factors		JUNB, TGFB1	LRP3

表1．オステミア（OstemiR）の発現パターン及びターゲット予測．miRNA の発現パターンから機能とターゲット mRNA が予測された．ヒトにおけるターゲット mRNA は，TargetScan 5.2 を用いて予測した．骨，幹性およびエピジェネティクスに関わるターゲット mRNA を列挙した．miR-16 及び miR-322/424 はターゲットを共有する．

る.

さらにヒートマップ解析とスキャッタープロット解析によって, OstemiR を抽出した(図4). miRNA PCR Array によって抽出された OstemiR について, 個別の定量 PCR によっても発現パターン解析を行った. まず miRNA Array の結果から, 内部標準を検討した結果, Snord66 が最も発現変動が少なかったためこれを KUSA 骨細胞分化系における内部標準とした. 個別の定量 PCR の結果, miR-21, miR-155, miR-322/424 については, 2つの実験系の間で, ほぼ同様の結果を得られ, データの信頼性が高まった. miR-16, miR-30d については, 2つの実験系の間で, 共通しない部分があった. 実験原理を踏まえて考察すると, miRNA PCR Array はスクリーニングとして網羅的解析に向いているものの, 細かな条件設定と検討には向かない. 個別の miRNA の定量のためには, より効率的でリニアな増幅が確認できる個別のリアルタイム PCR が向いている. したがって, 最終的にはリアルタイム PCR のデータのほうが信頼度が高い.

オステミアのターゲット予測

これまでの発現パターン解析によって, 特徴的な発現変動を示した miRNA について, その機能予測とターゲット予測を行った(表1). ターゲット予測によって, OstemiR は骨形成および幹細胞誘導に関わる遺伝子をターゲットとすることが予測された. またエピジェネティクスに関連する遺伝子も OstemiR のターゲットとして予測された. OstemiR のうち分化誘導に伴い発現上昇する miR-30d, miR-155, miR-21, miR-16 は, 骨芽細胞の分化マーカーであり, 未成熟な Osteoprogenitor を維持する因子を抑制する可能性がある. 骨細胞段階である 2w+ で発現上昇する miR-16, 34c は, 骨細胞マーカーであり, 骨細胞分化抑制性の骨芽細胞維持遺伝子を抑制する可能性がある.

骨細胞分化制御因子をターゲットとする miRNA の検索

骨芽細胞分化マーカーを標的とする miRNA を予測したところ, 脊椎動物間で広く保存された miRNA 認識部位, 哺乳類でのみ保存された miRNA 認識部位, 保存度の低い miRNA 認識部位がそれぞれ予測された. ここでは, 脊椎動物あるいは哺乳類で保存された miRNA およびその認識領域のみについて考察する. 骨細胞マーカーである dmp1 の 3' 非翻訳領域を認識する miRNA として let-7/98 が予測された. 今回の実験で, let-7 family のメンバーはいずれも骨細胞分化で発現低下したため, let-7 family の発現低下によって Dmp1 の発現抑制解除が起こったと考えられる.

CCN2/CTGF の mRNA 制御

骨芽細胞および軟骨細胞の分化促進因子である ctgf/ccn2 の 3'-UTR から予測された miRNA のうち, miR-18ab, miR-19 は OstemiR であり, 他に miR-26ab/1297, miR-132/212, miR-133 が予測された. ccn2/ctgf mRNA の 3' 非翻訳領域には CAESAR という遺伝子発現抑制領域があり (Kubota and Kondo, 2000; Eguchi and Kubota, 2001), またマウス (Kondo and Kubota, 2000) およびニワトリ (Mukudai and Kubota, 2005; 2008) の ccn2/ctgf にも遺伝子発現を負に調節する領域が示されてきた. 本研究の OstemiR として miR-18ab が抽出されたが, miR-18a は既にヒトにおいて ctgf/ccn2 mRNA に直接作用することが報告されている(Ohgawara and Kubota, 2009). また ctgf/ccn2 の遺伝子発現は, デキサメタゾンによって誘導されることが知られている(Dammeier and Beer, 1998; Kubota and Moritani, 2003), 本研究での骨誘導による ctgf/ccn2 の急激な発現上昇も同じ機序と考えられる. またデキサメタゾンによる ctgf/ccn2 発現誘導および抑制は, 既報の miR-18a および本研究で明らかとなった前述の複数の miRNA の作用によるものと考えられる.

Runx2 を制御する miRNA

骨芽細胞分化のマスター転写因子である Runx2 は, 分化誘導後 4h, 2d, 1w の時点で抑制されたが, 2w で発現が上昇した. Runx2 の 3' 非翻訳領域には2カ所の miR-30a/d/e 認識配列, および一カ所の miR-23ab 認識配列が予測され, それらは今回の実験で発現変動した OstemiR である. 他に miR-205, miR-218, miR-338, miR-106/302, miR-203, miR-217, miR-204/211 が予測された. 定量 PCR では miR-30d は 4h+で発現上昇するものの 2w+ではコントロールと同様の発現レベルであった. 従って, miR-30d は Runx2 の発現を抑制するが, miR-30d の発現が低下することで Runx2 の発現抑制の解除が起こると考えられる. miR-30a/e も Runx2 を標的とすると予測され, これらは 2w-で発現低下することから, miR-30 family は Runx2 を標的として骨の細胞分化に関与すると考えられる.

Runx2 を制御する miRNA として miR-30c, miR-135a, miR-204, miR-133a, miR-217, miR-

205, miR-34, miR-23a, miR-338 が立証されている(Zhang and Xie, 2011). それらの miRNA は Runx2 のタンパク質の発現を抑制するだけでなく, 3'-UTR のレポーターおよび ALP 活性をも抑制し, さらにそれらの Anti-miRNA は, Runx2 3'-UTR のレポーターを活性化した. 我々の実験においても miR-30a/d/e , miR-34c の発現が変動したため, Zhang らの報告でみられたように Runx2 の発現を抑制すると考えられる.

Osterix を制御する miRNA

もう一つの骨芽細胞分化のマスター転写因子 Sp7/Osterix の発現は, 1w+で著しく抑制されていた. Osterix を標的とすると予測された miRNA のうち, miR-96/1271, miR-125, miR-27ab は OstemiR であり, 他に miR-383, miR-145 が予測された. miR-27ab, miR-96, miR-125 は 2w-で発現上昇し, 特に miR-125 は 2w+で発現が低下した. Osterix の発現変動パターンはトリッキーではあるが, miR-96, 125, 27ab, miR-383, miR-145 による発現抑制と解除が推察される.

この他に, ヒト骨髄間質由来間葉系幹細胞から骨芽細胞への分化を制御する miRNA として miR-138 が報告されている(Eskildsen and Taipaleenmaki, 2011). miR-138 は FAK の制御を介して骨芽細胞分化を抑制する.

骨細胞分化に関わる転写因子群

骨芽細胞分化に Runx2 ならびに Osterix が必須であることが示されてきたが、後期分化、骨細胞分化に至る過程で機能する転写因子群は知られていない。本研究で新たに3つの転写因子を同定した。そのうち Mef2c は骨形成の阻害に関わる sost の遺伝子調節に関わる事が知られている。一方、これらの転写因子は前者の既知の転写因子とはことなり、他の組織や細胞でも発現しており、骨芽細胞では後期分化に寄与していると考えられる。一方、Runx2 は後期分化に対して抑制的に働いている。これまでに Runx2 の骨芽細胞での過剰発現マウスでは、この必須な役割にも関わらず、骨量の低下と骨細胞の喪失が報告されている(Liu et al., 2001)。また、Osterix は骨細胞での発現が高く、コンディショナルノックアウトマウスでは、骨細胞の異常や発現遺伝子の低下が観察されている(Zhou et al, 2010)。骨細胞は骨の恒常性に対して、骨代謝を制御するメタボロスタット的な役割を担っていることが考えられている事から(Watanabe and Ikeda, 2010), 単なる転写因子の導入による分化亢進ではなく, 適度(分化時期や状況)な発現調節が, 効率のよい骨の再生においても重要と思われる。この点においても miRNA の応用は有効であると考えられる。

E. 結論

本研究で明らかにされた OstemiR は, 今後の機能解析によって, 単数の miRNA あるいは anti-miRNA, もしくは複数の組み合わせによって, 骨芽細胞分化を正負に調節すると考えられる. miRNA はタンパク質や抗体と比べると小分子であるため, 比較的簡単かつ安価に合成および定量できる. また miRNA が細胞外に分泌されるという生物学的および医学的に重要な報告が増えている(Hu and Drescher, 2012). 従って, 本研究で同定した OstemiR および anti-ostemiR は, 生理的な骨代謝の理解に有用であると同時に, 歯周病と骨粗鬆症の診断および治療のために有用な新しい指標およびツールとなりうる.

F. 研究発表

1. 論文発表

Mukudai Y, Kubota S, Eguchi T, Sumiyoshi K, Janune D, Kondo S, Shintani S, Takigawa M. A coding RNA segment that enhances the ribosomal recruitment of chicken ccn1 mRNA. J Cell Biochem. 2010 Dec 15;111(6):1607-18.

Role of low-density lipoprotein receptor related protein 1 (LRP1) in CCN2/connective tissue growth factor (CTGF) protein transport in chondrocytes. Kawata K, Kubota S, Eguchi T, Aoyama E, Moritani NH, Kondo S, Nishida T, Takigawa M. J Cell Sci. 2012 Mar 27.

2. 学会発表

Eguchi T, Hattori T, Nakashima M, Matusita K, Tsuchiya Y. Molecular Chaperone HSP70 Induction by PEX Expression Vector. BMB2010. 第 33 回日本分子生物学会年会・第 83 回日本生化学会 合同大会, LBA(p), Kobe, 2010.12.7.

江口傑徳, 土屋由佳子. 骨芽細胞分化に関わる microRNAs の同定. 第5回エピジェネティクス研究会年会. 2011 年 5 月 19 日. 熊本.

Watanabe K, Aburatani H, Ikeda K
An in vitro model for osteocyte differentiation.

The 33rd Annual Meeting of the American Society for Bone & Mineral Research. Sep 18 San Diego, USA

G. 知的所有権の取得状況

1. 特許取得
なし
2. 実用新案登録
なし
3.その他
なし

研究成果の刊行に関する一覧表

研究成果の刊行に関する一覧表

書籍

著者氏名	論文タイトル名	書籍全体の編集者名	書 籍 名	出版社名	出版地	出版年	ページ
Watanabe K.	Classical models of senile osteoporosis	Duque G, Watanabe K	Osteoporosis Research	Springer-Verlag	London, UK	2011	115-121

雑誌

発表者氏名	論文タイトル名	発 表 誌	巻号	ページ	出版年
Kawata K, Kubota S, Eguchi T, Aoyama E, Moritani NH, Kondo S, Nishida T, Takigawa M.	Role of low-density lipoprotein receptor related protein 1 (LRP1) in CCN2/connective tissue growth factor (CTGF) protein transport in chondrocytes.	Journal of cell science	in press	in press	2012
Mukudai Y, Kubota S, Eguchi T, Sumiyoshi K, Janune D, Kondo S, Shintani S, Takigawa M.	A coding RNA segment that enhances the ribosomal recruitment of chicken ccn1 mRNA.	J Cell Biochem.	Dec 15;111(6):	1607-18.	2010

研究成果　別刷

ARTICLE
Journal of Cellular Biochemistry 111:1607–1618 (2010)
Journal of Cellular Biochemistry

A Coding RNA Segment That Enhances the Ribosomal Recruitment of Chicken *ccn1* mRNA

Yoshiki Mukudai,[1,2] Satoshi Kubota,[3*] Takanori Eguchi,[3] Kumi Sumiyoshi,[3] Danilo Janune,[3] Seiji Kondo,[2,3] Satoru Shintani,[2] and Masaharu Takigawa[1,3*]

[1]*Biodental Research Center, Okayama University Dental School, Okayama, Japan*
[2]*Department of Oral and Maxillofacial Surgery, Showa University Dental School, Tokyo, Japan*
[3]*Department of Biochemistry and Molecular Dentistry, Okayama University Graduate School of Medicine, Dentistry and Pharmaceutical Sciences, Okayama, Japan*

ABSTRACT

CCN1, a member of the CCN family of proteins, plays important physiological or pathological roles in a variety of tissues. In the present study, we initially found a highly guanine–cytosine (GC)-rich region of approximately 200 bp near the 5′-end of the open reading frame, which was always truncated by amplification of the corresponding cDNA region through the conventional polymerase chain reaction. An RNA in vitro folding assay and selective ribonuclease digestion of the corresponding segment of the *ccn1* mRNA confirmed the involvement of a stable secondary structure. Subsequent RNA electromobility-shift assays demonstrated the specific binding of some cytoplasmic factor(s) in chicken embryo fibroblasts to the RNA segment. Moreover, the corresponding cDNA fragment strongly enhanced the expression of the reporter gene in *cis* at the 5′-end, but did not do so at the 3′-end. According to the results of a ribosomal assembly test, the effect of the mRNA segment can predominantly be ascribed to the enhancement of transport and/or entry of the mRNA into the ribosome. Finally, the minimal GC-rich mRNA segment that was predicted and demonstrated to form a secondary structure was confirmed to be a functional regulatory element. Thus, we here uncover a novel dual-functionality of the mRNA segment in the *ccn1* open reading frame, which segment acts as a *cis*-element that mediates posttranscriptional gene regulation, while retaining the information for the amino acid sequence of the resultant protein. J. Cell. Biochem. 111: 1607–1618, 2010.

KEY WORDS: CCN FAMILY; CCN1; CYR61; POST-TRANSCRIPTIONAL REGULATION; RIBOSOME

CCN1 (Cyr61/CEF-10) is a cysteine-rich secretory protein, and a member of the "CCN family" [Lau and Lam, 1999; Brigstock et al., 2003; Perbal and Takigawa, 2005], which also includes CTGF/Fisp12 (CCN2) [Almendral et al., 1988; Bradham et al., 1991; Ryseck et al., 1991], Nov (CCN3) [Joliot et al., 1992], ELM-1/WISP-1 (CCN4) [Hashimoto et al., 1998; Pennica et al., 1998], CTGF-3/WISP-2/COP1 (CCN5) [Pennica et al., 1998; Zhang et al., 1998], and WISP-3 (CCN6) [Pennica et al., 1998]. Each of the CCN family proteins consists of four conserved modules, that is, the insulin-like growth factor-binding protein (IGFBP), von Willebrand factor type C repeat (VWC), thrombospondin type I repeat (TSP1), and carboxyl terminal (CT) modules. These modules are known to interact with a number of biomolecules to conduct extracellular signaling network that yields multiple effects on the development of a variety of tissues.

Cyr61, a human and mouse ortholog of CCN1, was first identified as a growth factor-inducible immediate-early response gene by differential hybridization screening of a cDNA library prepared from serum-stimulated mouse fibroblasts; [Lau and Nathans, 1985] and CEF-10, a chicken ortholog of CCN1 (cCCN1), was identified as a v-*src*-inducible gene in chicken embryo fibroblasts (CEF cells) [Simmons et al., 1989]. Thereafter, a number of biological functions of CCN1 were clarified. CCN1 enhances growth factor-stimulated cell migration [Kireeva et al., 1996, 1998; Babic et al., 1998] and mediates cell adhesion [Kireeva et al., 1996, 1997, 1998; Jedsadayanmata et al., 1999; Chen et al., 2001]. Recent reports revealed that CCN1 plays important roles in tumorigenesis or tumor suppression. Namely, CCN1 stimulates tumor progression of breast cancer [Tsai et al., 2000; Xie et al., 2001] and enhances the

Grant sponsor: Japan Society for the Promotion of Science; Grant numbers: 19109008, 21592360.
*Correspondence to: Satoshi Kubota and Masaharu Takigawa, Department of Biochemistry and Molecular Dentistry, Okayama University Graduate School of Medicine, Dentistry and Pharmaceutical Scicences, 2-5-1 Shikata-cho, Kita-ku, Okayama 700-8525, Japan. E-mail: kubota1@md.okayama-u.ac.jp; takigawa@md.okayama-u.ac.jp
Received 23 February 2010; Accepted 21 September 2010 • DOI 10.1002/jcb.22894 • © 2010 Wiley-Liss, Inc.
Published online 4 November 2010 in Wiley Online Library (wileyonlinelibrary.com).

malignant phenotype of a gastric adenocarcinoma cell line [Babic et al., 1998]. By contrast, it was also reported that expression of CCN1 is down-regulated in prostate cancer [Pilarsky et al., 1998] and leiomyoma [Sampath et al., 2001] and that overexpression of CCN1 suppresses cell proliferation associated with enhanced expression of p53 and $p21^{waf1}$ in non-small cell lung cancer cells [Tong et al., 2001]. Of note, the involvement of CCN1 in the induction of apoptosis has been described as well [Juric et al., 2009]. CCN1 also plays important roles in skeletal formation and acquisition of vascular integrity during fetal development [O'Brien and Lau, 1992]. Expression of *ccn1* is observed in developing cartilage and the circulatory system during embryogenesis [O'Brien and Lau, 1992], and CCN1 promotes the differentiation of murine limb bud mesenchymal cells into chondrocytes [Wong et al., 1997]. Finally, *ccn1*-null mice suffer embryonic death due to a failure of chorioallantonic fusion or placental vascular insufficiency and compromised vessel integrity [Mo et al., 2002]. As such, CCN1 displays various functions in physiological and/or pathological processes; however, the molecular mechanism of its gene expression, particularly that at the post-transcriptional level, still remains unclear.

Recent studies have demonstrated that post-transcriptional regulation of mRNA plays important roles in gene expression, as well as in transcriptional regulation and that *cis*-elements on mRNA and *trans*-factors in the cytoplasm and/or nuclei are involved in the regulation. A variety of mRNA regulatory *cis*-elements, such as adenine–uridine-rich elements (ARE) [Bevilacqua et al., 2003] and micro RNA targets [Siomi and Siomi, 2009] in a number of transcripts mediate post-transcriptional and translational gene regulation during the transport of mRNA from the nucleus to ribosome in the cytosol [St Johnston, 1995; Moallem et al., 1998] via the regulation of the stability of mRNA [Moallem et al., 1998] and translation efficiency [Siomi and Siomi, 2009]. Our recent studies also uncovered a *cis*-acting element of structure-anchored repression (CAESAR) and the 3′-100/50 element in the *ccn2* gene, which is another member of the CCN family [Kubota et al., 2000, 2005; Mukudai et al., 2005, 2008]. Most of these elements are reported to be present in 5′- and 3′-untranslated regions (UTRs) [Kubota et al., 1999]. However, certain RNA *cis*-elements are also present in the open reading frame (ORF) of several genes, such as those for interleukin 2 [Chen et al., 1998], thymidylate synthase [Lin et al., 2000], and manganese superoxide dismutase [Davis et al., 2001].

In the present study, we focused on a secondary-structured GC-rich region in the ORF of the chicken *ccn1* mRNA, and found that the region functions as a positive post-transcriptional *cis*-regulatory element of gene expression, by promoting the ribosomal entry of the *cis*-linked mRNA in a location-dependent manner.

MATERIALS AND METHODS

CELL CULTURE

CEF cells were isolated from a day-10 chicken embryo by trypsinization, and maintained in Dulbecco's modified Eagle's minimum essential medium supplemented with 10% fetal bovine serum in humidified air containing 5% CO_2 at 37°C, as described previously [Mukudai et al., 2003].

PURIFICATION OF TOTAL CELLULAR RNA AND REVERSE TRANSCRIPTASE-MEDIATED POLYMERASE CHAIN REACTION (RT-PCR)

Total RNA was isolated from sub-confluent CEF cells according to the method of Chomczynski and Sacchi [1987], and was treated with 250 μg/ml of protease K (Invitrogen, Carlsbad, CA) for 16 h in the final step of RNA preparation. Reverse transcription by avian myeloblastosis virus (AMV) reverse transcriptase was conducted by using a commercially available kit (Takara, Tokyo, Japan) with 1 μg of total RNA and random primers. The polymerase chain reaction (PCR) was carried out with a recombinant *Taq* DNA polymerase (Invitrogen), according to the manufacturer's protocol, in the presence or absence of "PCRx Enhancer Solution" attached as a supplement of the polymerase. Nucleotide sequences of the primers for amplification of the 5′-region of *ccn1* were 5′-CGC TAA GAC ATG GGC TC-3′ for the sense, and 5′-CCT CAG AAG CGT CCA GA-3′ for the anti-sense. These primers were designated "S-1" and "AS-1," respectively. The amplification cycle consisted of 30 s at 95°C, 30 s at 70°C, and 1 min at 72°C. After 35 cycles of chain reaction and subsequent incubation at 72°C for 5 min, the PCR products were analyzed by conducting 1% agarose gel electrophoresis.

The amplicons were subcloned into pGEM T-Easy (Promega, Madison, WI) by a TA-cloning method and sequenced. Among the clones, those yielding sense transcripts from the T7 bacteriophage promoter in the plasmid were utilized for subsequent in vitro transcription experiments.

DNA SEQUENCING AND COMPUTER ANALYSIS

The cDNAs subcloned into the respective plasmids were sequenced with a Big Dye Terminator Cycle Sequencing Ready Reaction Kit ver. 2.0 (Applied Biosystems, Foster City, CA), 1× SEQUENCERx Enhancer Solution A (Invitrogen) as a supplement, and an ABI PRISM 310 Genetic Analyzer (Applied Biosystems). DNA sequence alignments and RNA secondary structure predictions were made by using a commercial computer software package, GENETYX-MAC ver. 11, or GENETYX ver. 6.1.2 (Software Development, Tokyo, Japan).

PREPARATION OF NUCLEAR AND CYTOPLASMIC EXTRACTS (S-100)

The nuclear fraction and cytoplasmic fraction (S-100) of CEF cells were prepared according to a previously described protocol [Glickman and Ripley, 1984] with a slight modification. Sub-confluent CEF cells in 10-cm dishes were washed with phosphate-buffered saline (PBS), collected into 1 ml per dish of hypotonic buffer [10 mM HEPES (pH 7.9), 1.5 mM $MgCl_2$, 10 mM KCl, 1 μg/ml leupeptin (Sigma–Aldrich, St. Louis, MO), 1 μg/ml aprotinin (Sigma–Aldrich), and 0.5 mM ditiothreitol (DTT)], and chilled on ice for 10 min. Then, the cells were homogenized by 10 strokes in a Dounce homogenizer on ice, and centrifuged at 3,000*g* for 15 min at 4°C to obtain the crude cytoplasmic and nuclear fractions, respectively.

For purification of the nuclear fraction, the crude nuclear fraction was re-suspended in the same volume of a low-salt buffer [20 mM HEPES (pH 7.9), 25% glycerol, 1.5 mM $MgCl_2$, 0.02 mM KCl, 0.2 mM EDTA, 1 μg/ml leupeptin, and 1 μg/ml aprotinin], and was gently shaken for 10 min at 4°C. Afterwards, the same volume of a high-salt

buffer [20 mM HEPES (pH 7.9), 25% glycerol, 1.5 mM $MgCl_2$, 1.2 M KCl, 0.2 mM EDTA, 1 μg/ml leupeptin, and 1 μg/ml aprotinin] was added drop wise into the swollen nuclear suspension; and the suspension was gently shaken for an additional 30 min at 4°C. The soluble nuclear fraction was obtained as the supernatant after centrifugation at 25,000*g* for 30 min at 4°C. Finally, it was dialyzed against a moderate salt buffer [20 mM HEPES (pH 7.9), 20% glycerol, 0.2 mM KCl, and 0.5 mM EDTA] for 16 h at 4°C, and then stored at −80°C until used.

For preparation of the cytoplasmic fraction, a 0.11 volume of 10× cytoplasmic buffer [0.3 mM HEPES (pH7.9), 1.4 M KCl, and 30 mM $MgCl_2$] was added to the crude cytoplasmic fraction, and centrifuged at 10,000*g* for 1 h at 4°C. The supernatant gave the cytoplasmic fraction (S-100), which was dialyzed and frozen in the same way as the soluble nuclear fraction.

The protein concentrations of both fractions were determined with a BCA protein assay kit (Pierce, Rockford, IL), utilizing bovine serum albumin (BSA; Sigma–Aldrich) as a standard.

PREPARATION OF RNA IN RIBOSOMAL FRACTION

The ribosomal fraction of CEF cells was prepared as described earlier [Canceill and Ehrlich, 1996] with slight modification. Sub-confluent CEF cells were washed with PBS, collected in PBS, and centrifuged at 500*g* for 5 min at 4°C. The cell pellet was re-suspended in a lysis buffer [50 mM Tris–HCl (pH 7.4), 0.25 M sucrose, 25 mM KCl, 5 mM $MgCl_2$, 2 mM DTT, 100 units/ml RNase inhibitor (Takara), and 0.7% NP-40], chilled on ice for 4°C, and centrifuged at 750*g* for 10 min at 4°C. The supernatant was re-centrifuged at 12,500*g* for 10 min at 4°C. The secondary supernatant was transferred to a new tube, and a 0.32 volume of high-KCl solution [50 mM Tris–HCl (pH 7.4), 0.25 M sucrose, 2 M KCl, 5 mM $MgCl_2$, 2 mM DTT, and 100 units/ml RNase inhibitor] was added, in order to adjust the KCl concentration to 0.5 M. The solution was layered onto 1 ml of a sucrose cushion solution [50 mM Tris–HCl (pH 7.4), 1 M sucrose, 0.5 M KCl, and 5 mM $MgCl_2$], and centrifuged at 245,000*g* for 6 h at 4°C. The pellet (ribosomal fraction) was composed of ribosomal proteins, ribosomal RNAs, and ribosome-associated messenger RNAs. Then, RNAs in the ribosomal fraction were purified by using the same method as used for the purification of total cellular RNA. Involvement of comparable quality and quantity of 28s and 18s rRNAs in each ribosomal fraction was confirmed by agarose gel electrophoresis.

IN VITRO TRANSCRIPTION OF RNA

The in vitro transcription reaction was carried out with a commercial kit, Riboprobe Combination System Sp6/T7 (Promega) according to the manufacturer's protocol. The plasmids described in another subsection were linearized by *Spe*I, *Pvu*II, or *Nco*I, transcribed by Sp6 or T7 bacteriophage RNA polymerase for 1 h at 37°C in the presence of alpha-[^{32}P]CTP (Amersham Pharmacia, Backingham-shire, UK) or digoxigenin-11-UTP (Roche, Basel, Switzerland), and subjected to DNase digestion and spin-column (Amersham Pharmacia) purification [32]. Thereafter, the labeled transcripts were suspended in a Tris-borate EDTA (TBE)-urea sample buffer (45 mM Tris-borate, 45 mM boric acid, 1 mM EDTA, 2 M urea, 6% Ficoll, 0.005% bromophenol blue, and 0.005% xylene cyanol), heated at 95°C for 10 min, and cooled on ice. Then, the denatured RNAs were analyzed by conducting 6% polyacrylamide gel electrophoresis (PAGE) in the presence of 6 M urea in 1× TBE buffer. The gel was subsequently dried and autoradiographed, or processed for signal detection with a commercially available kit, following the manufacturer's indications (DIG Nucleic Acid Detection Kit; Roche). Unlabeled RNA transcripts were produced in a similar manner, but in the absence of labeled nucleotides. Schematic representations of the method and of the lengths of several transcripts are shown in Figure 2A.

RNA molecular size standards were produced by in vitro transcription of a mixture of RNA templates (Century Marker, Ambion, Austin, TX) in the presence of alpha-[^{32}P]CTP. The radiolabeled RNA transcripts were subjected to spin-column purification, and 1.5×10^4 cpm in total was used as an RNA molecular standard in each experiment.

RNA IN VITRO FOLDING AND ANALYTICAL RNASE PROTECTION ASSAYS

The RNA folding assay was carried out as described previously [Dignam et al., 1983; Odelberg et al., 1995] with a slight modification. Forty-thousand cpm or 100 ng of labeled RNA was heated at 95°C for 5 min, gradually cooled to room temperature, and then chilled at 4°C for more than 2 days in an RNA folding buffer [10 mM HEPES (pH 7.9), 40 mM KCl, 3 mM $MgCl_2$, 1 mM DTT, 0.5 mg/ml yeast tRNA (Boehringer Mannheim, Mannheim, Germany) and 0.5 mg/ml BSA], in order to allow the RNA to form a secondary structure. The folded RNAs were then digested with 1 μl of 100-fold diluted RNase T1 solution (1,000 units/μl, Ambion) for 10 min at 37°C. After phenol/chloroform extraction, the digested RNAs were precipitated by 2.5 M ammonium acetate and ethanol at −30°C for 2 h. The RNA pellets were dissolved in a TBE-urea sample buffer and then subjected to 6% TBE-urea PAGE as described in another subsection.

RNA ELECTROMOBILITY SHIFT ASSAY (REMSA)

The nuclear or cytoplasmic extract containing 0–10 μg of protein was incubated at 25°C for 30 min with 40,000 cpm of radio-labeled RNA in 19 μl of a binding buffer [5 mM HEPES (pH 7.9), 7.5 mM KCl, 0.5 mM $MgCl_2$, 0.1 M EDTA, 0.5 mM DTT, and 0.1 mg/ml BSA] containing 0.1 mg/ml of yeast tRNA to rule out non-specific interaction. Then, the binding mixture was incubated with 1 μl of 100-fold diluted RNase Cocktail (Ambion) for a further 10 min at 37°C. The RNA–protein complex was subjected to 6% native PAGE in 0.5× TBE buffer. The gel was subsequently dried and autoradiographed.

For competition experiments, proteins were pre-incubated with 0–100 ng of unlabeled competitor RNA for 30 min at 25°C, followed by incubation with the radio-labeled RNA for another 30 min at 25°C.

WESTERN BLOTTING ANALYSIS

The nuclear and cytoplasmic proteins were separated in a 12% SDS–PAGE gel, and then transferred to polyvinylidene difluoride membrane (Hybond-P; Amersham Pharmacia). The blot was blocked with 5% skim milk in Tris-buffered saline (TBS) for 16 h at 4°C. The blot was next incubated with a 1/2,000 dilution of monoclonal anti-

alpha tubulin antibody (Sigma–Aldrich) or 1/1,000 dilution of monoclonal anti-lamin B1 antibody (Zymed, South San Francisco, CA) in TBS containing 0.05% Tween 20 (TBS-T) for 1 h at 37°C and, thereafter, incubated with a 1/20,000 dilution of peroxidase-conjugated goat anti-mouse IgG antibody (American Qualex, La Mirada, CA) in TBS-T for 1 h at 37°C. Subsequently, the immunosignals were visualized with an ECL Western Blotting Analysis System (Amersham Pharmacia).

PLASMID CONSTRUCTS

The SV40 promoter-driven firefly luciferase expression plasmid (pGL3; Promega) was modified by inserting multiple cloning sites at the downstream end of the luciferase gene, as described in our previous studies [Kubota et al., 1999, 2000]; and this plasmid, designated pGL3L(+), was used to elucidate the *cis*-acting effects of the *ccn1* fragment. A HSV-TK promoter-driven *Renilla*-luciferase expression plasmid (pRL-TK; Promega) was used as an internal control for transfection experiments to monitor the transfection efficiency. The 5′ cDNA fragment of *ccn1* was obtained by PCR. For ligation at the upstream end of the luciferase gene, a sense primer (5′-AAG CTT GGG CTC TGC GGG AGC TCG-3′) and anti-sense primer (5′-CCA TGG TCT CCC CTC AGA CTG TGC TC-3′) were prepared. The sense and anti-sense primers contained flanking *Hin*dIII and *Nco*I sites, respectively; hence the amplicon was double-digested with *Hin*dIII site and *Nco*I, purified, and subcloned between the corresponding sites in pGL3L(+). On the other hand, for the insertion of the fragment at the upstream end of the luciferase gene, the sense primer (5′-TCT AGA TGG GCT CTG CGG AGC C-3′) and anti-sense primer (5′-GAA TTC TCC CCT CAG ACT GTG CTC-3′) were designed to contain flanking *Xba*I and *Eco*RI sites, respectively. Thus, the amplicon was double-digested with these enzymes, purified, and subcloned between the corresponding sites in pGL3L(+). For the construction of the plasmids expressing the minimal structured segment of 209 bases fused to the luciferase mRNA, four long oligonucleotides were synthesized and assembled between the unique *Hin*dIII and *Nco*I sites in pGL3L(+), utilizing the internal *Pvu*II site in the *ccn1* cDNA fragment. On the way to the construction of this plasmid, pGL3-RPC, two derivatives were also obtained as intermediate products. These plasmids, designated pGL3-RPF and pGL3-RPL, contain the former *Hin*dIII–*Pvu*II and latter *Pvu*II–*Nco*I subfragments of the minimal segment, respectively. These short cDNA segments were also subcloned into pGEM3Zf(−) (Promega) for in vitro transcription of RNAs with SP6 or T7 RNA polymerase. The structures of the newly constructed plasmids were confirmed by restriction enzymatic digestion and nucleotide sequencing analyses.

DNA TRANSFECTION

Two-hundred thousand CEF cells were seeded into a 35-mm tissue culture dish 24 h before transfection. Cationic liposome-mediated DNA transfection was carried out with 1 μg of each pGL3L(+) derivative in combination with 0.5 μg of pRL-TK, according to the manufacturer's methodology (Lipofectamine; Invitrogen). Forty-eight hours after the transfection, the cells were lysed in 500 μl of a passive lysis buffer (Promega); and then the cell lysate was directly used for the luciferase assay.

LUCIFERASE ASSAY

The dual luciferase assay system (Promega) was applied for the sequential measurement of firefly (reporter) and *Renilla* (transfection efficiency standard) luciferase activities with specific substrates of beetle luciferin and coelenterazine, respectively. Quantification of both luciferase activities and calculation of relative ratios were carried out manually with a luminometer (TD20/20: Turner Designs, Sunnyvale, CA), as described in our earlier study [Kubota et al., 1999].

QUANTITATIVE RNASE PROTECTION ASSAY

For preparation of the probe for the firefly luciferase gene transcript, pGL3L(+) was double-digested with *Hin*dIII and *Xba*I. The resulting 1.7-kbp fragment containing the firefly luciferase gene was separated in 1% agarose gel, excised, purified, and subcloned between the corresponding sites in pGEM3Zf(+) (Promega). The plasmid was linearized by *Hin*cII, and in vitro transcription was carried out by using T7 bacteriophage RNA polymerase, as described in another subsection. The length of the probe was approximately 400 nt.

RNase protection assays were carried out with a commercial kit (RPA II kit, Ambion), according to the manufacturer's protocol. Twenty-four hours after the transfection of CEF cells, total cellular or ribosome-fractional RNA was prepared, as described in another subsection. Two micrograms of RNAs was hybridized with the radio-labeled firefly luciferase probe, digested by the RNase cocktail, and precipitated in ethanol. The recollected RNA was subjected to 6% TBE-urea PAGE. Thereafter, the gels were dried and autoradiographed.

RESULTS

A HIGHLY GC-RICH SEGMENT IN THE ORF OF THE CCN1 cDNA AS INDICATED BY TRUNCATION DURING PCR

Initially, RT-PCR was carried out with CEF RNA, in order to simply obtain a cDNA fragment corresponding to the upstream end of the ORF of *ccn1*, which was predicted to be 600-bp in length (Fig. 1). However, to our surprise, the length of the resultant amplicon was

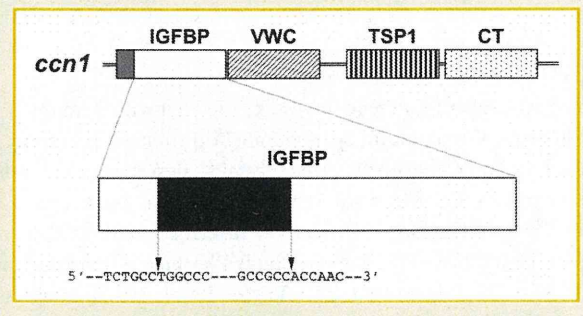

Fig. 1. Schematic representation of the cDNA structure of chicken *ccn1* and the truncated area. The entire cDNA structure that is composed of a signal peptide-encoding region (gray box) and module-encoding regions are shown at the top. An enlarged illustration is also provided for the IGFBP region to specify the approximate location of the truncated region of 209 bp and the nucleotide sequences at the boundaries.

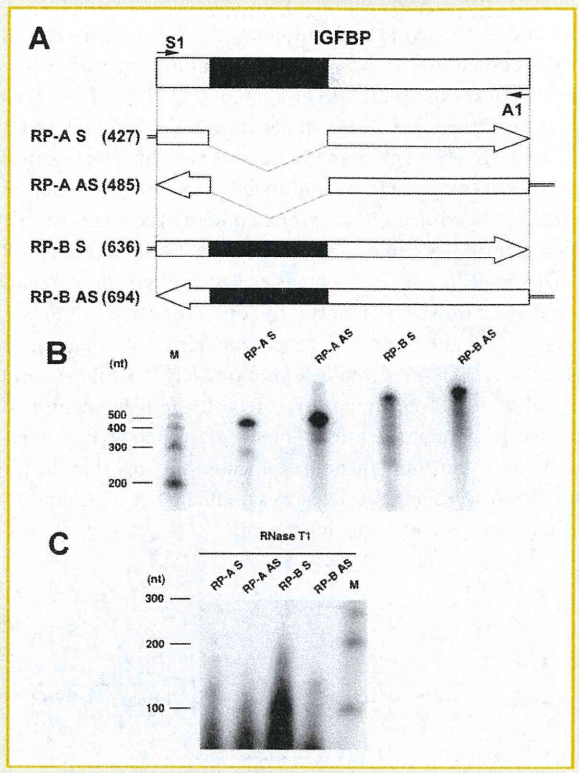

Fig. 2. In vitro transcription and analysis of folding of *ccn1* mRNA segments. A: Schema for preparation of radiolabeled RNAs in vitro. The structures of each transcription template and the resultant transcripts are shown as combined illustrations. The amplicons of RT-PCR were subcloned into pGEM T-Easy (Promega) for in vitro transcription of the corresponding RNAs. The names of transcripts are shown therein. Prior to the transcription reaction, the plasmids were linearized, and transcription was carried out by using T7 or SP6 RNA polymerase for sense (S) or anti-sense (As) transcripts, respectively. The orientation of transcription and sizes of transcripts are denoted. Double lines represent nucleotide sequences originating from the vector. B: Analysis by use of 6% PAGE of the transcribed RNAs shown in panel A. M represents RNA molecular size markers, produced by in vitro transcription of a mixture of RNA templates (Century Marker, Ambion), and the sizes of the transcripts are indicated at the left of the panel. C: Susceptibility of the *ccn1* mRNA fragments to RNase T1 after folding. Radio-labeled RNAs were heated at 95°C, gradually cooled to room temperature, and thereafter cooled further to 4°C, in order to allow them to self-fold. Then, the folded RNAs were digested with RNase T1. After digestion, the RNAs were purified through phenol extraction, precipitated with ethanol and ammonium sulfate, and separated by denaturing 6% PAGE. M refers to RNA molecular size markers, with sizes indicated at the left of the panel. The data in panel B and C are representative of two separate experiments with similar results.

approximately 400 bp, which was 200 bp shorter than that expected. In contrast, in the presence of PCRx Enhancer Solution, which is a reagent that facilitates the amplification of GC-rich sequences, an amplicon with the expected length was obtained.

To confirm their identity, these 400 and 600-bp amplicons, which were designated RP-A and RP-B, respectively, were subcloned into pGEM T-Easy vector by a TA-cloning method, and sequenced (Fig. 1). The nucleotide sequence of RP-B was exactly the same as that of the *ccn1* reported in GenBank (accession number: J04496) by Simmons et al. In contrast, the nucleotide sequence of RP-A lacked an internal 209-bp portion, and the GC-content of the deleted region was particularly high (73.5%). These findings firmly indicate a novel GC-rich segment in the ORF of *ccn1* cDNA, which is suspected to yield a secondary-structured mRNA segment.

SECONDARY STRUCTURE FORMATION OF RP-B RNA IN VITRO

In order to examine whether or not this region was able to actually form a stable secondary structure on mRNA through internal base-pairing, we carried out RNA in vitro transcription for use in an RNA in vitro folding assay. Figure 2A illustrates the length and orientation of the radio-labeled RNA corresponding to each RT-PCR amplicon (RP-A or RP-B). On 6% TBE-urea PAGE, the radio-labeled transcripts gave single bands of expected electromobility, as shown in Figure 2B, indicating proper RNA synthesis in all of the samples. Thereafter, the RNAs were subjected to extensive RNA in vitro folding assays using digestion with RNase. The RNAs were heat-denatured, and gradually cooled, in order to allow them to form a secondary structure, and then, incubated with RNase T1, which digests single-stranded RNA at "G" (Fig. 2C). Both the sense and anti-sense (negative control) of RP-A were digested almost completely, leaving only small (<50 nt) and faint bands corresponding to the undigestable region. However, the sense strand of RP-B was partially protected from digestion, leaving discrete bands of >100 nt, which indicates double-stranded regions resistant to RNase T1 digestion. Interestingly, the anti-sense strand of RP-B was digested almost completely, in contrast to the sense strand. These results indicate the existence of a stable secondary structure through internal base-pairing in the 5′ region of *ccn1* mRNA, further suggesting a capability of acting as a *cis*-element in the regulation of *ccn1*.

DIRECT BINDING OF CYTOSOLIC FACTOR(S) TO THE STRUCTURED REGION OF CCN1 mRNA

In general, protein counterparts are required for an element to regulate gene expression. Therefore, by utilizing RNA electromobility shift assay (REMSA) methodology, we next investigated the existence of a possible *trans*-factor protein(s) that could bind to this putative *cis*-element. As shown in Figure 3A, incubation of the folded sense-strand RNA of the corresponding region (RP-B S) with 5–10 μg of the cytoplasmic extract from CEF cells resulted in the retardation of the RNA in the gel. In contrast, no shifted band was observed after the incubation of the sense-strand RNA from the cDNA region with the internal 209-nt deletion (RP-A S), either with the nuclear or cytoplasmic extract, indicating that the interaction depended upon the 209-nt region. Western blotting analysis (Fig. 3A) revealed that lamin B1 (a marker of the nuclear fraction) and alpha-tubulin (a marker of the cytoplasmic fraction) were present only in the nuclear and cytoplasmic extract, respectively, confirming no cross contamination between each fraction. Furthermore, pre-incubation with unlabeled folded competitor RNA abolished the formation of a complex between RP-B S and cytoplasmic protein (Fig. 3B). Together with the fact that all binding reactions were carried out in the presence of 190 ng of non-specific tRNA, this result indicates that the interaction of the cytoplasmic protein with RP-B S RNA fragment was specific.

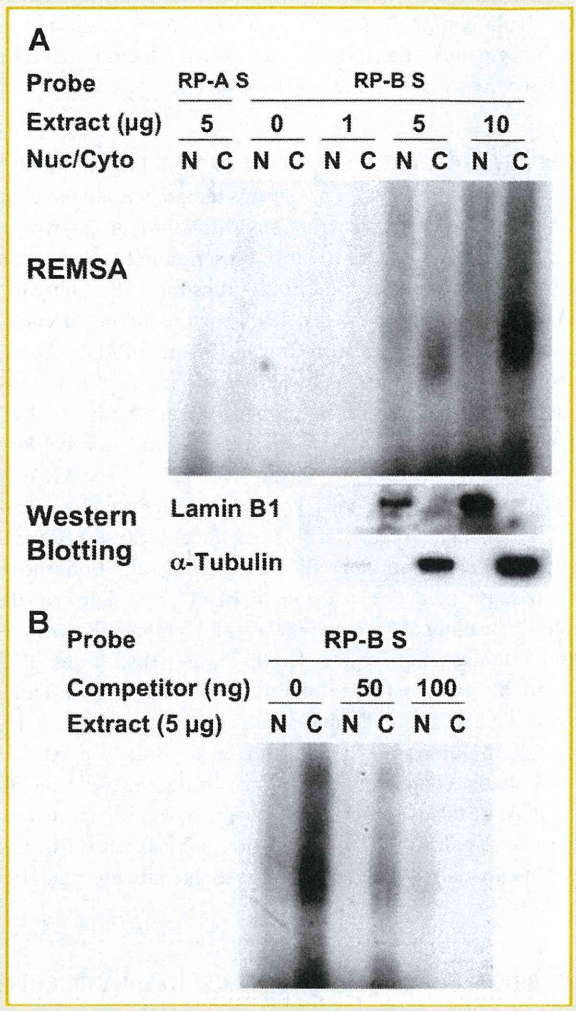

Fig. 3. Binding profile of chicken nuclear or cytosolic factors to the *ccn1* RNA segments, as evaluated by RNA gel electromobility shift assays (REMSA). A: Binding analysis of the *ccn1* mRNA segments to nuclear or cytosolic protein. The radio-labeled and folded RNA probes (RP-A S or RP-B S) were incubated with 0, 1, 5, or 10 μg of nuclear (N) or cytosolic (C) protein extract. After RNase digestion, the complex was subjected to 6% native PAGE. Western blotting analysis of the lamin or alpha-tubulin in the indicated amount of the extract was also performed to confirm successful subcellular fractionation in these experiments. B: Competition analysis to confirm the specificity of the interaction. Five micrograms of nuclear (N) or cytosolic (C) protein extract was pre-incubated with 0–100 ng of unlabeled RP-B S RNA as a competitor, followed by incubation with radio-labeled RNA probe (RP-B S). After RNase digestion, the complex was subjected to 6% native PAGE. The data in both panels are representative of two separate experiments, yielding comparable results.

THE RP-B FRAGMENT OF CCN1 cDNA-ENHANCED GENE EXPRESSION IN CIS

The results described in the previous subsection suggest the collaboration of the 5′-end ORF portion of *ccn1* mRNA and the cytoplasmic binding protein to exert post-transcriptional regulation of *ccn1*. Therefore, we evaluated the validity of this hypothesis by employing a system of chimeric firefly luciferase fusion gene constructs [Kubota et al., 1999, 2000; Mukkudai et al., 2003]. Initially, RP-B cDNA was minimally modified by deleting the "ATG" initiation codon to avoid translation interference and inserted in the sense direction at the 5′- or 3′-end of the firefly luciferase gene in a parental expression plasmid, pGL3L(+) (Fig. 4A). The resultant plasmid constructs were designated pGL3-5′-RPB′ and pGL3-3′-RPB′, respectively. The parental and two chimeric expression plasmids were subjected to a calibrated transient expression assay using CEF cells, with *Renilla* luciferase (pRL-TK) co-expression as an internal control. As demonstrated in Figure 4B, both pGL3-5′-RPB′ and pGL3-3′-RPB′ enhanced reporter gene activity in comparison with pGL3(+). However, importantly, the fragment RP-B located at the 5′-end of the reporter gene enhanced the reporter gene expression much more strongly (approximately 3.5-fold vs. control) than that at the 3′-end (approximately 1.5-fold vs. control). The difference in enhancing effects on the reporter gene expression between these two chimeric genes indicates not only that the 5′-end of the ORF of *ccn1* mRNA acted as an enhancing *cis*-element, but also that the effect was site dependent.

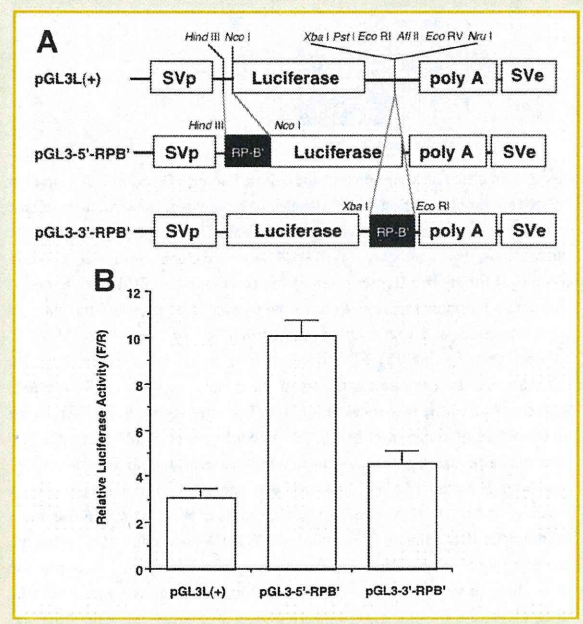

Fig. 4. *cis*-enhancing activity of RP-B S on reporter gene expression. A: Structures of the plasmids utilized in this evaluation. The pGL3L(+) was derived from pGL3-control vector (Promega), as described previously (Kubota et al., 1999, 2000; Mukudai et al., 2003) and contains restriction enzyme cleavage sites as indicated. Both pGL3-5′-RPB′ and pGL3-3′-RPB′ were derived from pGL3L(+), and thus, the basic structure of every plasmid was the same. In pGL3-5′-RPB′, RP-B cDNA was inserted between *Hin*dIII and *Nco*I sites upstream of the firefly luciferase gene. On the other hand, in pGL3-3′-RPB′, RP-B cDNA was inserted between *Xba*I and *Eco*RI sites, downstream of the firefly luciferase gene. Abbreviations: SVp, SV40 promoter; SVe, SV40 enhancer; polyA, SV40 polyadenylation signal; Luciferase, firefly luciferase gene. B: Firefly luciferase activities from the plasmid in panel A in CEF cells. CEF cells were co-transfected with one of the plasmids in panel A and pRL-TK (Promega: as an internal control). After 2 days, a Dual Luciferase Assay (Promega) was carried out. Activity levels are represented as relative values of the measured luminescence of firefly luciferase versus *Renilla* luciferase. Mean values of the results of three experiments are displayed with error bars of standard deviations.

EFFECTS OF THE RP-B FRAGMENT ON THE RIBOSOMAL ASSEMBLY OF LINKED mRNA

It is now recognized that RNA *cis*-elements play important roles in post-transcriptional regulation in collaboration with nuclear and/or cytosolic *trans*-factor protein(s) at various stages, such as stabilization or destabilization of mRNA, transportation from the nucleus to the cytosol and ribosomal entry of mRNAs. Based on this knowledge and the results of the reporter gene assay (Fig. 4), we evaluated the effect of the fragment of *ccn1* mRNA on the ribosomal association of mRNA. The total RNA and ribosomal RNA fractions of the CEF cells, into which the chimeric constructs described in the previous subsection were transfected, were subjected to an RNA protection assay, with a 400-nt RNA of the firefly luciferase gene probe (Fig. 5). As a result, total luciferase mRNA level was significantly, but modestly (<2-fold) increased by the addition of the RP-B fragment at the 5′-end, whereas it enhanced the ribosomal association of the reporter gene mRNA much more strongly. Indeed, it was fivefold higher than the control value and was consistent with the result of the reporter gene assay. In contrast, RP-B fragment at the 3′-end conferred no significant effect on the ribosomal entry of the *cis*-lined luciferase RNA. These results indicate the RP-B segment to function as a post-transcriptional regulatory segment that predominantly enhances the ribosomal association of the mRNA when located *in cis* at the 5′-end.

SECONDARY STRUCTURE OF THE GC-RICH REGION IN THE RP-B SEGMENT

In order to further confirm the secondary structure formation and to analyze the structure actually formed in solution, we performed an RNase T1 protection analysis of the RP-B segment. Unless forming a secondary structure, the *cis*-regulatory element was anticipated to highly susceptible to RNase T1 digestion, since it was characterized by quite high GC-content. As observed in Figure 6A, the anti-sense form of the RP-B segment was digested into small pieces by RNase T1. In contrast, three major RNA fragments of 50–100 bases in the RP-B sense transcript were resistant to RNase T1, whereas no longer than 22 base fragment can be expected without secondary structure. To gain more insight into the structure of the *cis*-regulatory element in the RP-B segment, we analyzed the region truncated through regular PCR in the initial experiments in silico. The computer program predicted that this region would form a stable secondary structure through internal base-pairing; indeed more than 65% of the bases in this region would be able to be paired by hydrogen bonds (Fig. 6B). Thus, it was strongly suspected that the protected RNA segments observed in Figure 6A could originate in this minimal GC-rich segment. In order to confirm this point, we repeated analytical RNase protection assay with the minimal RNA segment (RPC) and its subfragments (RPF and RPL; Fig. 6C). Consequently, an RNA segment in RPC was distinctly protected from RNase T1 digestion. In contrast, RPL, the latter-half subfragment of RPC was totally degraded by the RNase. It should be noted that an RNA segment in RPF, the former-half fragment was also protected. As such, these major bands were anticipated to originate in the two stem loops formed at the upstream side of the GC-rich region. These findings further provided a structural basis for this segment to function as an RNA *cis*-regulatory element.

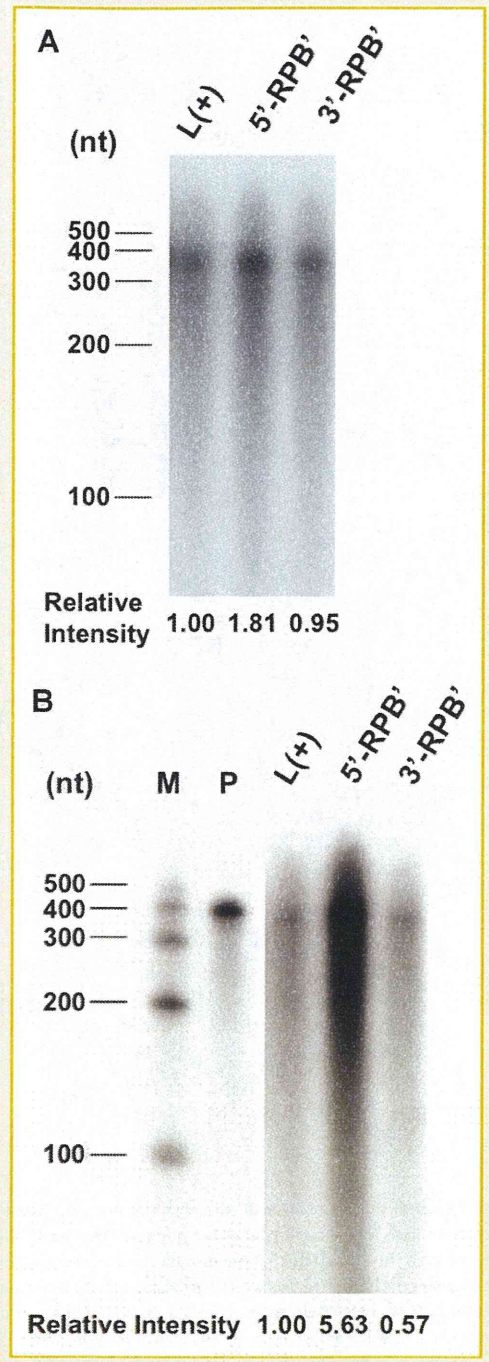

Fig. 5. RNase protection analysis of the luciferase mRNAs with or without RP-B expressed in CEF cells. CEF cells were transfected with each plasmid shown in Figure 4. After 2 days, total RNA (A) and the ribosomal fraction RNA (B) were collected and purified (see Materials and Methods section). Two micrograms of each RNA was subjected to the RNase protection assay. The free probe (P) and protected probe fragments of each sample were separated by denaturing 6% PAGE. M represents RNA molecular size markers, with the sizes indicated at the left of the panel. Relative ribosome-associated mRNA levels versus that of L(+) are shown below the autoradiogram. The data are representative of three separate experiments.

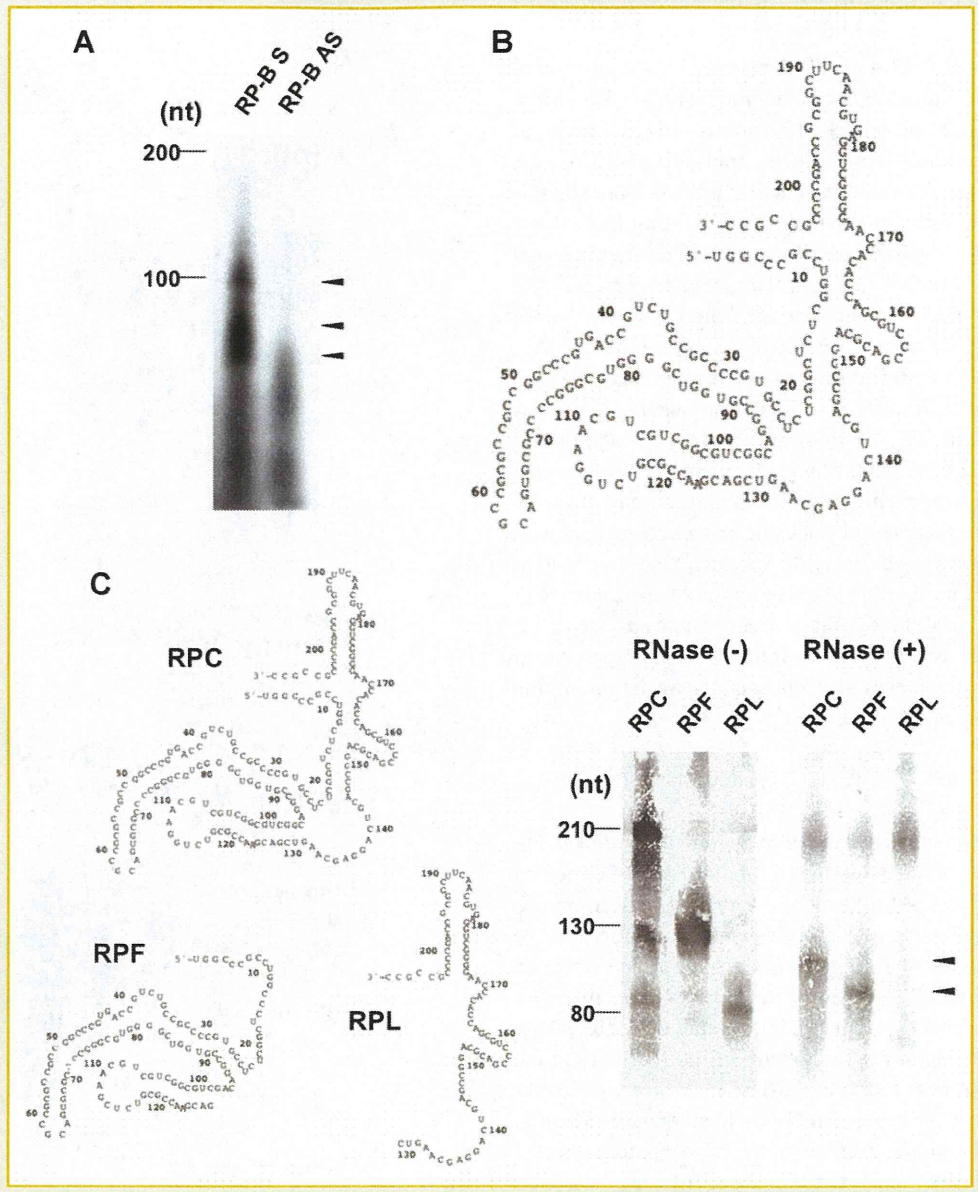

Fig. 6. Secondary structure of the GC-rich region. A: Analytical RNase protection assay of the folded RP-B RNA segment. Three major protected RNA fragments in denaturing gel electrophoresis are indicated by arrowheads (right). Positions of RNA chain-length markers are shown at the left. B: Predicted secondary structure of the 209-base region truncated during RT-PCR of the RP-B segment. Numbers are counted from the upstream boundary of the amplified and truncated areas. C: RNase protection assay of the minimal GC-rich region and its subfragments. Left panel represents the RNA structures of the entire 209-base region and its subfragments. Each in vitro transcribed RNA was folded and subjected to denaturing gel electrophoresis with or without RNase T1 digestion, which is displayed in the right panel. Approximate chain lengths of the undigested RNAs are given at the left, while protected bands are pointed by arrowhead at the right.

EVOLUTIONARY CONSERVATION OF THE GC-RICH REGION AMONG VERTEBRATES

Generally, important nucleotide sequences are highly conserved among species that need the function of the corresponding regions. In this context, we compared the cDNA sequences of the GC-rich region in the *ccn1* gene among chick, mouse and human species. Alignment of the three sequences clearly indicated that the GC-rich region has been highly conserved during the evolution of vertebrates (Fig. 7A). This is partly because these sequences are involved in the ORF encoding CCN1. However, the results of maximum-matching analysis in comparison with those of the other ORF regions clearly indicated that the GC-rich region has been further conserved. Indeed, the matching score was 7–8% higher in the GC-rich regions than the others (Fig. 7B). These findings suggest the functional significance of the GC-rich segment in the natural context, at least in vertebrates.

FUNCTIONAL CONFIRMATION OF THE MINIMAL STRUCTURED REGION AS A REGULATORY ELEMENT

Finally, to examine if the GC-rich structured region of 209 bases was necessary and sufficient to enhance gene expression *per se*, the